# Measurement of Pancharatnam's phase by robust interferometric and polarimetric methods

J. C. Loredo,[1] O. Ortíz,[1] R. Weingärtner,[1,2] and F. De Zela[1]
[1]*Departamento de Ciencias, Sección Física, Pontificia Universidad Católica del Perú, Apartado, Lima 1761, Peru*
[2]*Department of Materials Science 6, University of Erlangen-Nürnberg, Martensstrasse 7, 91058 Erlangen, Germany*
(Received 17 April 2009; published 24 July 2009)

We report on theoretical calculations and experimental observations of Pancharatnam's phase originating from arbitrary SU(2) transformations applied to polarization states of light. We have implemented polarimetric and interferometric methods, which allow us to cover the full Poincaré sphere. As a distinctive feature, our interferometric array is robust against mechanical and thermal disturbances, showing that the polarimetric method is not inherently superior over the interferometric one, as previously assumed. Our strategy effectively amounts to feeding an interferometer with two copropagating beams that are orthogonally polarized with respect to each other. It can be applied to different types of standard arrays, such as a Michelson, a Sagnac, or a Mach-Zehnder interferometer. We exhibit the versatility of our arrangement by performing measurements of Pancharatnam's phases and fringe visibilities that closely fit the theoretical predictions. Our approach can be easily extended to deal with mixed states and to study decoherence effects.

DOI: 10.1103/PhysRevA.80.012113 PACS number(s): 03.65.Vf, 03.67.Lx, 42.65.Lm

## I. INTRODUCTION

As is well known, Pancharatnam's phase was originally introduced to deal with the relative phase of two polarized light beams [1]. It anticipated geometrical phases that are nowadays intensively studied both theoretically and experimentally. Among all geometrical phases, Berry's phase [2] has played a major role in prompting the upsurge of a vast amount of investigations dealing with topological phases in quantum and classical physics. Berry's phase was originally introduced by considering the adiabatic evolution of a quantum state subjected to the action of a parameter-dependent Hamiltonian. However, the first experiments aiming at exhibiting such a phase were performed with classical states of light, using cw lasers [3]. It was soon realized that the phase tested in such experiments differed from Berry's phase, as it was larger than the latter by a factor of 2. The reason for this was that the experimentally studied phase [3] arose from SO(3) instead of SU(2) transformations. Indeed, Tomita and Chiao [3] let polarized light pass a coiled optical fiber and measured the phase originated from the adiabatic change suffered by the propagation direction of a light beam. Thus, the corresponding parameter space being explored—the sphere of directions—differed from the parameter space that was involved in Berry's original phase. The latter was Bloch sphere, on which any spin-1/2 state can be represented. Another two-state system formally equivalent to a spin-1/2 state is a polarized light, in which, e.g., vertically ($V$) and horizontally ($H$) polarized states constitute the counterparts of the spin-up and spin-down quantum states. Polarization states can be represented on the Poincaré sphere, which is equivalent to the Bloch sphere. An early experiment testing the appearance of Pancharatnam's phase in polarization states describing closed paths on the Poincaré sphere was the one performed by Bhandari and Samuel [4]. This interferometric test was however restricted to a limited set of SU(2) transformations and, moreover, some of the transformations used by the authors were nonunitary, as they employed linear polarizers to bring the polarization back to its initial value. Thus, Chyba *et al.* [5] performed alternative tests by employing only unitary transformations to exhibit Pancharatnam's phase, although such transformations were still restricted to cover a limited SU(2) range. In spite its original formulation in terms of polarization states of light, Pancharatnam's phase has not been fully exhibited in optical implementations, in contrast to more recent experiments based on neutron spin interferometry [6–8]. Some years ago, Wagh and Rakhecha [9,10] proposed two alternative methods to measure Pancharatnam's phase. One method is based on a polarimetric procedure, while the other is an interferometric one. Both procedures have been tested and compared against one another in experiments using neutrons [6,7]. The conclusion drawn from these experiments was that the polarimetric method is inherently superior over the interferometric method. This is so mainly because the polarimetric method is insensitive to mechanical and thermal disturbances that usually plague interferometric methods. Neutron interferometry, in particular, is also limited through spatial constraints that are imposed by the geometry of the monocrystals used to construct the interferometers. In order to explore a large range in the parameter space of the geometric phase, people contrived to realize some regions of this space by electrically inducing phase changes that were beyond the range accessible through rotation of a flipper. However, such a procedure prompted some criticisms [11] concerning the parameter spaces that were involved in the two phase evolutions, as one of them was physically obtained by the rotation of a flipper and the other by electrical means. On the other hand, the allegedly more accurate polarimetric method allows phase measurements only modulo $\pi$ and is therefore unable to verify certain features such as the anticommutation of Pauli matrices, e.g., $\sigma_x\sigma_y=-\sigma_y\sigma_x$, which is something that was beautifully done with the interferometric method [6].

To the best of our knowledge, the two methods referred to above have not yet been tested against each other in all-optical experiments being capable of exploring the full parameter range of the Poincaré sphere. We have thus endeavored to compare both methods of measuring Pancharatnam's phase by using all-optical setups. In this work we present a

 

robust interferometric arrangement that makes the full range of SU(2) polarization transformations accessible. Furthermore, we have also implemented a polarimetric array with a similar coverage, so that both methods could be compared against each other. As we shall see, our interferometric arrangement is insensitive to mechanical and thermal disturbances. This represents an important improvement, as compared to conventional interferometric arrangements. The latter are usually set up as a variant of a Michelson, a Mach-Zehnder, or a Sagnac interferometer. Our method works with any of these variants, so that one could choose the most appropriate arrangement. For example, one could explore decoherence effects by measuring geometric phases in polarization single-photon mixed states using Mach-Zehnder interferometers, similarly to recently reported experiments [12]. In such a case, the fringe contrast (visibility) of the interferometric pattern also conveys information about the geometric phase. Although our work deals with pure states only, we have also tested the visibility of our patterns as a function of SU(2) transformations, obtaining very good agreement with theoretical predictions.

Our experiments, in addition to test Pancharatnam's phase with great versatility, serve the purpose of showing a common ground for classical and quantum manifestations of topological phases. Indeed, although our tests have been performed with classical states of light, they could be straightforwardly extended to experiments with single photons. Our theoretical discussion has thus been couched in a quantum-mechanical language, so that, e.g., the polarization states of classical light are represented by kets like $|V\rangle$ and $|H\rangle$. It should thus be clear that the features under study are not of an intrinsic classical or quantum-mechanical nature. Instead, it is the topological aspect that manifests itself as a common ground for both classical and quantum phenomena.

The paper is organized as follows. In Sec. II we review the interferometric and the polarimetric methods for measuring Pancharatnam's phase and derive theoretical results that apply in our case. In Sec. III we describe our experimental arrangements and present our results, comparing them with our theoretical predictions. Finally, we present in Sec. IV our conclusions.

## II. INTERFEROMETRIC AND POLARIMETRIC METHODS

Given two states, $|i\rangle$ and $|f\rangle$, their Pancharatnam's relative phase $\Phi_P$ is defined as $\Phi_P=\arg\langle i|f\rangle$. A very direct way to exhibit $\Phi_P$ is through interferometry. Indeed, consider two interfering nonorthogonal states $|i\rangle$ and $|f\rangle$, with $|i\rangle \neq |f\rangle$. If we apply a phase shift $\phi$ to one of the states, the resulting intensity pattern is given by

$$I = |e^{i\phi}|i\rangle + |f\rangle|^2 = 2 + 2|\langle i|f\rangle|\cos(\phi - \arg\langle i|f\rangle). \quad (1)$$

The maxima of $I$ are thus attained at $\phi=\arg\langle i|f\rangle=\Phi_P$. We are interested in exhibiting $\Phi_P$ in two-level systems and when Pancharatnam's phase arises as a consequence of having submitted an initial state $|i\rangle$ to an arbitrary transformation $U \in \mathrm{SU}(2)$ that converts it into a final state $|f\rangle=U|i\rangle$. The intensity measurement for which Eq. (1) applies can be implemented with the help of, say, a Mach-Zehnder interferometer. Alternatively, one could employ polarimetric methods. We will discuss both methods in what follows. But before, and for later reference, let us introduce the two parametrizations of $U \in \mathrm{SU}(2)$ that we shall use in our analysis. We call them the *YZY* and the *ZYZ* forms for obvious reasons: the first one is given by

$$U(\xi,\eta,\zeta) = \exp\left(-i\frac{\xi}{2}\sigma_y\right)\exp\left(i\frac{\eta}{2}\sigma_z\right)\exp\left(-i\frac{\zeta}{2}\sigma_y\right), \quad (2)$$

while the second form is given by

$$U(\beta,\gamma,\delta) = \exp\left[i\left(\frac{\delta+\gamma}{2}\right)\sigma_z\right]\exp(-i\beta\sigma_y)\exp\left[i\left(\frac{\delta-\gamma}{2}\right)\sigma_z\right] = \begin{pmatrix} e^{i\delta}\cos\beta & -e^{i\gamma}\sin\beta \\ e^{-i\gamma}\sin\beta & e^{-i\delta}\cos\beta \end{pmatrix}. \quad (3)$$

To pass from one form of $U$ to the other, one needs to connect the respective parameters. The corresponding equations of transformation involve, generally, trigonometric formulas, so that the different parameters are not connected to one another through algebraic relations [16]. The representation of Eq. (3) is particularly well adapted to exhibit Pancharatnam's phase. Indeed, taking as initial state $|i\rangle=|+\rangle_z$, i.e., the eigenstate of $\sigma_z$ that belongs to the eigenvalue of +1, and setting $|f\rangle=U|+\rangle_z$ we have

$$\langle i|f\rangle = {}_z\langle +|U(\beta,\gamma,\delta)|+\rangle_z = e^{i\delta}\cos\beta. \quad (4)$$

From the definition of Pancharatnam's phase, i.e., $\Phi_P=\arg\langle i|f\rangle$, we obtain $\Phi_P=\delta+\arg(\cos\beta)$, for $\beta \neq (2n+1)\pi/2$. Because $\cos\beta$ can take on positive and negative real values, $\arg(\cos\beta)$ equals 0 or $\pi$. Hence, $\Phi_P$ is defined modulo $\pi$. In any case, the parametrization $U(\beta,\gamma,\delta)$ of Eq. (3) is seen to be most appropriate to exhibit $\Phi_P=\delta$ (modulo $\pi$). On the other hand, for the optical implementation of $U$, the parametrization of the *YZY* form is more appropriate. Indeed, it is well known [13] that with the help of three retarders, viz., two quarter-wave plates and one half-wave plate, it is possible to implement any $U \in \mathrm{SU}(2)$ in the polarization space of, e.g., horizontally and vertically polarized states of light: $\{|H\rangle,|V\rangle\}$. This requires that one represents $U$ in the form given by Eq. (2), i.e., the *YZY* form, because of the following relationship involving the Euler angles $\theta_1,\theta_2,\theta_3$ (see, e.g., [14]):

$$\exp[-i(\theta_3+3\pi/4)\sigma_y]\exp[i(\theta_1-2\theta_2+\theta_3)\sigma_z] \times\exp[i(\theta_1-\pi/4)\sigma_y] = Q(\theta_3)H(\theta_2)Q(\theta_1). \quad (5)$$

Here, $Q$ means a quarter-wave plate and $H$ means a half-wave plate. The arguments of the retarders are the angles of their major axes to the vertical direction. In the case of a $U$ given by Eq. (2), by applying Eq. (5) we obtain

$$U(\xi,\eta,\zeta) = Q\left(\frac{-3\pi+2\xi}{4}\right)H\left(\frac{\xi-\eta-\zeta-\pi}{4}\right)Q\left(\frac{\pi-2\zeta}{4}\right). \quad (6)$$

Having discussed the two parametrizations of $U \in \mathrm{SU}(2)$ that are useful for our purposes, we turn now to the implementa-

tion of the experimental arrangements that allow us to exhibit Pancharatnam's phase.

### A. Interferometric arrangement: Mach-Zehnder and Sagnac

In general, with an interferometric array Pancharatnam's phase can be drawn from intensity measurements that are essentially described by Eq. (1). If we introduce $U$ as given in Eq. (2) into Eq. (1), we obtain the intensity as

$$I = \left| \frac{1}{\sqrt{2}}[e^{i\phi}|+\rangle_z + U(\xi,\eta,\zeta)|+\rangle_z] \right|^2$$
$$= 1 - \cos\left(\frac{\eta}{2}\right)\cos\left(\frac{\xi+\zeta}{2}\right)\cos(\phi)$$
$$- \sin\left(\frac{\eta}{2}\right)\cos\left(\frac{\xi-\zeta}{2}\right)\sin(\phi). \quad (7)$$

From Eqs. (2) and (3) it follows that the parameters of these two representations of $U \in \mathrm{SU}(2)$ are related through $\tan(\delta)=\tan(\frac{\eta}{2})\cos(\frac{\xi-\zeta}{2})/\cos(\frac{\xi+\zeta}{2})$. Hence, $I$ can be written as

$$I = 1 - \cos\left(\frac{\eta}{2}\right)\cos\left(\frac{\xi+\zeta}{2}\right)\sec(\delta)\cos(\delta-\phi), \quad (8)$$

making it evident that an interferometric method for exhibiting $\Phi_P$ would require measuring the shift induced by $U$ on the intensity pattern by an angle $\delta=\Phi_P$ (modulo $\pi$). Now, the expression for $I$ as given in Eq. (8) is somewhat inconvenient, because it mixes $\delta$ with parameters of a representation to which it does not belong. By expressing Eq. (8) with the parameters of $U(\beta,\gamma,\delta)$, we obtain

$$I = 1 - \cos(\beta)\cos(\delta-\phi), \quad (9)$$

thus rendering clear that the visibility $v \equiv (I_{\max}-I_{\min})/(I_{\max}+I_{\min})$ is given by $v=\cos\beta$, i.e., it is independent of Pancharatnam's phase. In terms of the parameters $\xi,\eta,\zeta$ the square of the visibility is given by

$$v^2(\xi,\eta,\zeta) = \tfrac{1}{2}[1+\cos\xi\cos\zeta-\cos\eta\sin\xi\sin\zeta]. \quad (10)$$

For experimental tests, it will be useful to write the visibility in terms of the angles of the retarders as follows:

$$v^2(\theta_1,\theta_2,\theta_3) = \frac{1}{2}\left[1+\cos\left(\frac{3\pi+4\theta_3}{2}\right)\cos\left(\frac{\pi-4\theta_1}{2}\right)\right.$$
$$-\cos(2\theta_1-4\theta_2+2\theta_3)$$
$$\left.\times\sin\left(\frac{3\pi+4\theta_3}{2}\right)\sin\left(\frac{\pi-4\theta_1}{2}\right)\right]. \quad (11)$$

Let us now refer specifically to a Mach-Zehnder interferometer. In order to calculate its output intensity, let us represent light beams as a superposition of polarization states ($\{|H\rangle,|V\rangle\}$) and momentum (or "which way," i.e., spatial) states ($\{|X\rangle,|Y\rangle\}$). These last states denote the two-way alternative that can be ascribed to the Mach-Zehnder interferometer. Let us consider first that our initial state is taken to be a vertically polarized state that enters the first beam splitter along the $X$ direction (e.g., the beam passing polarizer $P_1$ in Fig. 1). It is represented by $|VX\rangle \equiv |V\rangle\otimes|X\rangle$. The actions of beam splitters, mirrors, and phase shifters are represented by operators in the two-qubit space with basis $\{|VX\rangle,|VY\rangle,|HX\rangle,|HY\rangle\}$. They act on the $|X\rangle,|Y\rangle$ states, leaving the polarization states $|H\rangle,|V\rangle$ unchanged. The actions of a 50:50 beam splitter and a mirror are given, respectively, by [14]

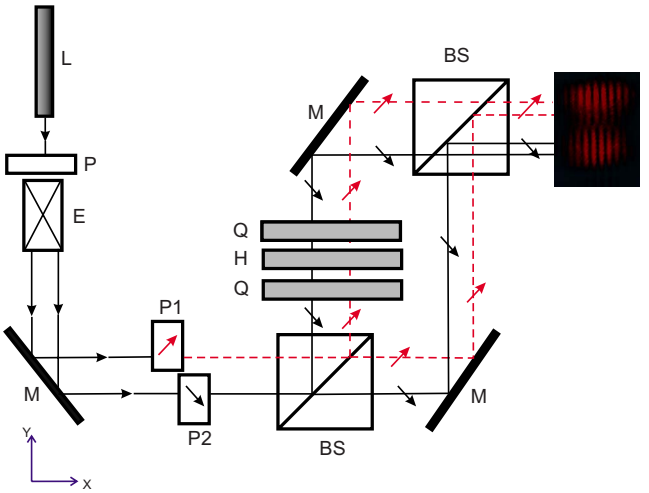


FIG. 1. (Color online) Interferometric arrangement for testing Pancharatnam's phase $\Phi_P$. Light from a He-Ne laser ($L$) passes a polarizer ($P$) and enters a beam expander ($E$), after which half of the beam goes through one polarizer ($P_1$) and the other half goes through a second polarizer ($P_2$), orthogonally oriented with respect to the first. The two collinear beams feed the same Mach-Zehnder interferometer (BS: beam splitter; $M$: mirror) in one of whose arms an array of three retarders has been mounted ($Q$:quarter-wave plate; $H$: half-wave plate), so as to realize any desired SU(2) transformation. This transformation introduces a Pancharatnam's phase $\Phi_P=\delta$ on one half of the beam and an opposite phase $\Phi_P=-\delta$ on the other perpendicularly polarized half, so that the relative phase of the two halves equals $2\delta$. From the relative shift between the upper and the lower halves of the interferogram that is captured by a CCD camera set at the output of the array, one can determine $\Phi_P$. Any instability of the array affects both halves of the interferogram in the same way, so that the relative shift of $2\delta$ is insensitive to instabilities.

$$U_{BS} = 1_P \otimes \frac{1}{\sqrt{2}}(|X\rangle\langle X| + |Y\rangle\langle Y| + i|X\rangle\langle Y| + i|Y\rangle\langle X|), \quad (12)$$

$$U_{mirr} = 1_P \otimes [-i(|X\rangle\langle Y| + |Y\rangle\langle X|)], \quad (13)$$

where $1_P$ means the identity operator in polarization space. Let us stress that the above expressions for the actions of a beam splitter and a mirror hold true irrespective of the fact that the spatial qubits are realized by classical or by quantum fields (see, e.g., [15]). Working with classical fields, the usage of kets (and bras) is just a useful mathematical means to represent field amplitudes [16]. Accordingly, a phase factor in one or in the other arm of the interferometer can be represented by $U_X(\phi)=1_P\otimes(\exp(i\phi)|X\rangle\langle X|+|Y\rangle\langle Y|)$ and $U_Y(\phi)=1_P\otimes(|X\rangle\langle X|+\exp(i\phi)|Y\rangle\langle Y|)$, respectively. If we mount an

array of retarders on, say, arm $X$ of the interferometer, its action would be represented by $U_P^X = U \otimes |X\rangle\langle X| + 1_P \otimes |Y\rangle\langle Y|$, where $U \in \mathrm{SU}(2)$ means the respective polarization transformation that the retarders produce, in our case the one given in Eq. (2). Similarly, $U_P^Y = 1_P \otimes |X\rangle\langle X| + U \otimes |Y\rangle\langle Y|$. For the arrangement shown in Fig. 1 we obtain

$$U_T = U_{BS} U_{mirr} U_X(\phi) U_P^Y U_{BS}. \tag{14}$$

This $U$ acts on the initial state $|VX\rangle$ and the intensity measured at one of the output ports of the final beam splitter is obtained by projecting the resulting state, $U_T|VX\rangle$, with the appropriate projectors: $|VX\rangle\langle VX|$ and $|HX\rangle\langle HX|$, thereby obtaining the vectors $|VX\rangle\langle VX|U_T|VX\rangle$ and $|HX\rangle\langle HX|U_T|VX\rangle$, respectively. Squaring the respective amplitudes and summing up we get the intensity as $I_V = |\langle VX|U_T|VX\rangle|^2 + |\langle HX|U_T|VX\rangle|^2$. A straightforward calculation yields

$$I_V = \frac{1}{2}\left[1 - \cos\left(\frac{\eta}{2}\right)\cos\left(\frac{\xi+\zeta}{2}\right)\cos(\phi) - \sin\left(\frac{\eta}{2}\right)\cos\left(\frac{\xi-\zeta}{2}\right)\sin(\phi)\right]. \tag{15}$$

As already shown, this can be written as

$$I_V = \tfrac{1}{2}[1 - \cos(\beta)\cos(\phi - \delta)]. \tag{16}$$

Using the above result, a direct measurement of Pancharatnam's phase $\delta = \Phi_P$ (modulo $\pi$) becomes possible: all one needs to do is to measure the fringe shift between two interferograms, with one of them serving as the reference ($\delta = 0$) and the other being obtained after applying the $U$ transformation. The practical problem with this method is the instability of the interferometric array. Minute changes in any component of the interferometer preclude an accurate determination of $\delta$. Different strategies can be applied to overcome this kind of shortcomings. Mechanical and thermal isolations of the arrangement is the most direct one, but it makes measurements rather awkward. Damping instabilities by a feedback mechanism is another possibility; but it makes the arrangement more involved and difficult to operate. A third option would be to use a Sagnac instead of a Mach-Zehnder interferometer. In a Sagnac-like interferometer one can make the two beams pass the same optical elements, so that any instability would affect both beams equally. One should then design the interferometer in such a way that the $U$ transformation acts on one beam alone, so that the other can serve as the reference beam. In our case, for reasons explained in detail in Sec. III, we turned to a different option that is based on the following observations.

Equation (16) holds for an initial state that is vertically polarized. When the initial state is horizontally polarized, then the intensity is given by

$$I_H = \tfrac{1}{2}[1 - \cos(\beta)\cos(\phi + \delta)]. \tag{17}$$

We observe that intensities $I_V$ and $I_H$ are shifted with respect to each other by $2\delta$. Thus, we can exploit this fact for measuring $\delta$. To this end, we polarize one half—say the upper half—of the laser beam vertically and the lower half horizontally. With such a beam we feed our interferometer. It can be mounted either in a Mach-Zehnder or in a Sagnac configuration. In both cases we can capture at the output an interferogram, half of which corresponds to $I_V$ and the other half corresponds to $I_H$. The upper fringes of the output will be shifted with respect to the lower ones by $2\delta$. As both halves of the beam pass the same optical elements, they will be equally affected by whatever perturbations. The array is therefore insensitive to instabilities. We thus need only to accurately measure the relative fringe shift in each interferogram in order to obtain $\delta$. By applying this method, we have measured Pancharatnam's phase with an accuracy that is similar to that reached by the polarimetric method, on which we turn next.

### B. Polarimetric arrangement

The optical setup for the polarimetric method, as proposed by Wagh and Rakhecha [9], is somewhat more demanding as compared to the interferometric method. At first sight, however, the polarimetric method could appear to be the simpler of the two options, because it requires a single beam, from which one extracts phase information. It is not obvious that phase information can be extracted from a single beam. However, the polarimetric method is in fact based on an analogous principle as the interferometric one, and in a certain sense polarimetry could be seen as "virtual interferometry." Let us briefly discuss how it works.

Consider an initial polarized state $|i\rangle = |+\rangle_z$ and submit it to the action of a $\pi/2$ rotation around an axis perpendicular to the polarization axis ($z$), e.g., a rotation around the $x$ axis. As a result, we obtain the state $(|+\rangle_z - i|-\rangle_z)/\sqrt{2}$. If we now phase shift this state by applying to it the operator $\exp(-\phi\sigma_z/2)$, we obtain the state

$$\begin{aligned} V|+\rangle_z &\equiv \exp(-i\phi\sigma_z/2)\exp(-i\pi\sigma_x/4)|+\rangle_z \\ &= (e^{-i\phi/2}|+\rangle_z - ie^{i\phi/2}|-\rangle_z)/\sqrt{2} \\ &= e^{-i\phi/2}(|+\rangle_z - ie^{i\phi}|-\rangle_z)/\sqrt{2}. \end{aligned}$$

We have thus generated a relative phase $\phi$ between the states $|+\rangle_z$ and $|-\rangle_z$, which is something analogous to what is achieved in an interferometer by changing the length of one of the two optical paths. Subsequently, we let $U$ act and as a result we obtain the state $UV|+\rangle_z = (e^{-i\phi/2}U|+\rangle_z - ie^{i\phi/2}U|-\rangle_z)/\sqrt{2} \equiv |\chi_+\rangle + |\chi_-\rangle$. It is from this last state that we can extract Pancharatnam's phase by intensity measurements. In order to accomplish this goal, we project $|\chi_+\rangle + |\chi_-\rangle$ on the state $V|+\rangle_z$, i.e., the phase-shifted split state we prepared before applying $U$. The corresponding intensity we measure is thus given by

$$I = |{}_z\langle + |V^\dagger(|\chi_+\rangle + |\chi_-\rangle)|^2. \tag{18}$$

Let us write $V|+\rangle_z = (e^{-i\phi/2}|+\rangle_z - ie^{i\phi/2}|-\rangle_z)/\sqrt{2} \equiv |\varphi_+\rangle + |\varphi_+\rangle$ and take $U$ as given by $U(\beta, \gamma, \delta)$ of Eq. (3). Calculating the amplitude ${}_z\langle +|V^\dagger(|\chi_+\rangle + |\chi_-\rangle) = (\langle\varphi_+| + \langle\varphi_-|)(|\chi_+\rangle + |\chi_-\rangle)$, we obtain, using $\langle\varphi_\pm|\chi_\pm\rangle = \exp(\pm i\delta)\cos(\beta)/2$ and $\langle\varphi_\mp|\chi_\pm\rangle = i\exp[\mp i(\gamma+\phi)]\sin(\beta)/2$, that $(\langle\varphi_+| + \langle\varphi_-|)(|\chi_+\rangle + |\chi_-\rangle) = \cos(\beta)\cos(\delta) + i\sin(\beta)\cos(\gamma+\phi)$ and, hence, that the intensity amounts to

$$I = \cos^2(\beta)\cos^2(\delta) + \sin^2(\beta)\cos^2(\gamma + \phi). \tag{19}$$

Equation (19) contains Pancharatnam's phase $\delta=\Phi_P$ (modulo $\pi$) in a form that allows its extraction through intensity measurements. Indeed, we observe from Eq. (19) that the minimal and the maximal intensities are given by $I_{\min}=\cos^2(\beta)\cos^2(\delta)$ and $I_{\max}=\cos^2(\beta)\cos^2(\delta)+\sin^2(\beta)$, respectively, so that

$$\cos^2(\delta)=\frac{I_{\min}}{1-I_{\max}+I_{\min}}, \tag{20}$$

which is the expression on which the polarimetric method is finally based.

A concrete experimental arrangement requires that we implement $V$ and $U$ with the help of retarders. To begin with, $\exp(-i\pi\sigma_x/4)=Q(\frac{\pi}{4})$ and $\exp(-i\phi\sigma_z/2)=Q(\frac{\pi}{4})H(\frac{\phi-\pi}{4})Q(\frac{\pi}{4})$. Using $Q^2(\frac{\pi}{4})=H(\frac{\pi}{4})$ and $\exp(+i\phi\sigma_z/2)=Q(-\frac{\pi}{4})H(\frac{\phi+\pi}{4})\times Q(-\frac{\pi}{4})$, we obtain

$$\begin{aligned}U_{tot}&\equiv V^{\dagger}UV\\&=H\left(-\frac{\pi}{4}\right)H\left(\frac{\phi+\pi}{4}\right)Q\left(-\frac{\pi}{4}\right)\\&\quad\times UQ\left(\frac{\pi}{4}\right)H\left(\frac{\phi-\pi}{4}\right)H\left(\frac{\pi}{4}\right).\end{aligned} \tag{21}$$

As for $U$, it is convenient to employ the form $U(\xi,\eta,\zeta)$ of Eq. (2), a form which can be directly translated into an arrangement with retarders, according to Eq. (6), i.e., an arrangement of the form $QHQ$. Inserting this $QHQ$ for $U$ into Eq. (21), we end up with an arrangement that consists of nine plates. In order to reduce the number of plates, we apply relations such as, e.g., $Q(\alpha)H(\beta)=H(\beta)Q(2\beta-\alpha)$, $Q(\alpha)H(\beta)H(\gamma)=Q(\alpha+\pi/2)H(\alpha-\beta+\gamma-\pi/2)$. The final reduction gives an array that consists of five retarders:

$$\begin{aligned}U_{tot}&=Q\left(-\frac{3\pi}{4}-\frac{\phi}{2}\right)Q\left(-\frac{5\pi+2\xi}{4}-\frac{\phi}{2}\right)\\&\quad\times Q\left(-\frac{9\pi+2(\xi+\eta)}{4}-\frac{\phi}{2}\right)H\left(-\frac{7\pi+\xi+\eta-\zeta}{4}-\frac{\phi}{2}\right)\\&\quad\times Q\left(-\frac{\pi}{4}-\frac{\phi}{2}\right).\end{aligned} \tag{22}$$

Note that such an arrangement could be implemented by mounting five plates having a common rotation axis, so that all the plates can be rotated simultaneously by the same angle $\phi/2$. The intensity that we should measure at the detector depends on $\xi$, $\eta$, and $\zeta$ according to the following expression:

$$\begin{aligned}I&=|\langle_z+|U_{tot}|+\rangle_z|^2\\&=\cos^2\left(\frac{\eta}{2}\right)\cos^2\left(\frac{\xi+\zeta}{2}\right)\\&\quad+\left[\cos\left(\frac{\eta}{2}\right)\sin\left(\frac{\xi+\zeta}{2}\right)\cos(\phi)\right.\\&\quad\left.+\sin\left(\frac{\eta}{2}\right)\sin\left(\frac{\xi-\zeta}{2}\right)\sin(\phi)\right]^2.\end{aligned} \tag{23}$$

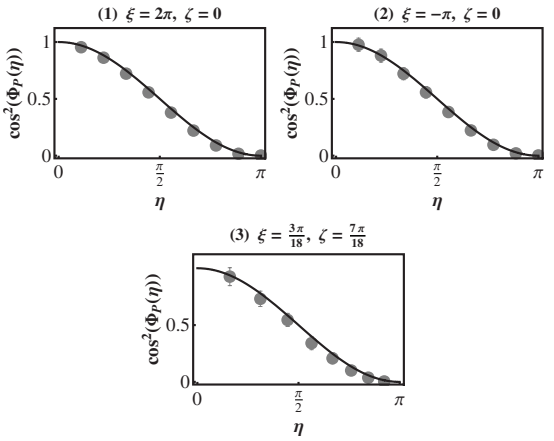


FIG. 2. Experimental results from a polarimetric measurement of Pancharatnam's phase. The upper graphs correspond to an array that consists of three retarders set in the forms $QQH$ (left) and $QHQ$ (right). Parameter values are as indicated and $\cos^2(\Phi_P)$ was measured as a function of $\eta$. The lower curve corresponds to the full array of five retarders set in the form $QQQHQ$.

From this intensity we can extract Pancharatnam's phase, as given by Eq. (20). We have tested this theoretical prediction under restricted conditions by manually rotating the retarders. Thus, we fixed $\zeta$ to $2\pi$, so that $\cos^2(\delta)=I_{\min}(1-I_{\max}+I_{\min})^{-1}=\cos^2(\eta/2)$ for all $\xi$. In such a case, Pancharatnam's phase (modulo $\pi$) should be given by $\Phi_P=\eta/2$. For $\zeta=2\pi$ the arrangement that realizes the corresponding $U_{tot}$ reduces to the following expression:

$$U_{tot}^{\xi=2\pi}=Q(\phi)Q\left(-\frac{\xi}{2}+\phi\right)H\left(\frac{\eta-\xi}{4}+\phi\right), \tag{24}$$

in which we have redefined the rotation angle $\phi$ according to $(-3\pi-2\phi)/4\rightarrow\phi$. If we instead fix $\xi=-\pi$, it still remains true that $\cos^2(\delta)=I_{\min}(1-I_{\max}+I_{\min})^{-1}=\cos^2(\eta/2)$, this time for all $\zeta$, so that $\Phi_P=\eta/2$ (modulo $\pi$) as before. The corresponding arrangement of retarders is now given by

$$\begin{aligned}U_{tot}^{\xi=-\pi}&=Q\left(\frac{3\pi+2\eta-2\phi}{4}\right)H\left(\frac{-4\pi+\zeta+\eta-2\phi}{4}\right)\\&\quad\times Q\left(\frac{-\pi-2\phi}{4}\right).\end{aligned} \tag{25}$$

It is worth noting that the intensity in this case is given by

$$I=\cos^2\left(\frac{\zeta}{2}\right)\cos^2\left(\frac{\eta-2\phi}{2}\right)+\sin^2\left(\frac{\zeta}{2}\right)\cos^2\left(\frac{\eta}{2}\right). \tag{26}$$

Setting $\eta=0$, $\zeta=\pi$, the intensity has a constant value, which is useful for adjusting the arrangement. The results of our measurements, including those corresponding to the full array with five retarders, are shown in Fig. 2. As one can see, they confirm the theoretical predictions within experimental errors.

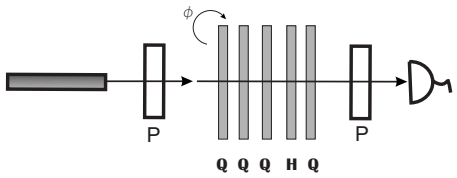


FIG. 3. Polarimetric arrangement for testing Pancharatnam's phase $\Phi_P$. With an array of five retarders ($Q$:quarter-wave plate; $H$: half-wave plate) and two polarizers ($P$), a relative phase $\phi$ between two polarization components $|\pm\rangle_z$ can be introduced, on which any desired SU(2) transformation can be applied. The five retarders are simultaneously rotated, thereby varying $\phi$, and the intensity $I(\phi)$ is recorded. From the maximum and the minimum values of $I$ one can determine $\Phi_P$, according to $\cos^2(\Phi_P)=I_{\min}/(1-I_{\max}+I_{\min})$.

## III. EXPERIMENTAL PROCEDURES AND RESULTS

### A. Polarimetric measurements

We have carried out measurements of the Pancharatnam phase by applying the polarimetric and the interferometric methods presented in the previous sections. In both cases the light source was a 30 mW cw He-Ne laser (632.8 nm). The polarimetric arrangement shown in Fig. 3 could have been designed so that the five retarders [see Eq. (22)] could be simultaneously rotated by the same amount. If one aims at systematically measuring Pancharatnam's phase with the polarimetric method, this would require having a custom-made apparatus on which one can mount the five plates with any desired initial orientation and then submit the whole assembly to rotation. As our aim was to simply exhibit the versatility of the method and to compare its accuracy with that of the interferometric method, we mounted a simple array of five independent retarders, so that each one of them could be manually rotated. With such an approach it takes some hours of painstaking manipulation to record all necessary data, whenever the experiment is performed with the full array of five retarders. For this reason, we initially restricted our tests to three retarders. This could be achieved by lowering the degrees of freedom, i.e., by fixing one of the three Euler angles, as explained in the previous section [see Eqs. (24) and (25)]. Having made measurements with three plates, we performed an additional run of measurements with the full arrangement of five retarders. Our results are shown in Fig. 2. They correspond to intensity measurements obtained with a high-sensitivity light sensor (Pasco CI-6604, Si PIN photodiode with spectral response in the range 320–1100 nm). As expected (retarders and polarizers could be oriented to within $1^0$), the experimental values are within 3–6 % in accordance with the theoretical predictions, depending on the number of retarders being employed.

### B. Interferometric measurements

We used two interferometric arrangements. One of them was a Mach-Zehnder interferometer and the other was a Sagnac interferometer. We started by mounting both interferometers in the standard way, but adding an array of three retarders on one arm for implementing any desired $U \in \mathrm{SU}(2)$. Usually, phase shifts $\phi$, as appearing in Eq. (9), originate from moving one mirror with, e.g., a low-voltage piezotransducer. One can then record the interference pattern by sensing the light intensity with a photodiode set at one of the output ports of the exiting beam splitter. Alternatively, one can capture the whole interference pattern with a charge-coupled device (CCD) camera. The Mach-Zehnder interferometer is easier to mount in comparison to the Sagnac interferometer. However, it has the disadvantage of being more unstable against environmental disturbances, thus requiring the application of some stabilizing technique such as, e.g., a feedback system. In contrast, the Sagnac interferometer is very stable with respect to mechanical and thermal disturbances. Nevertheless, mounting a Sagnac interferometer can be difficult for geometrical reasons. By using one or the other method, one can obtain two interferograms—one with and the other without the retarders in place. In our case, capturing the whole interference pattern with a CCD camera—instead of sensing it with a photodiode—proved to be the most convenient approach with both arrangements, Mach-Zehnder and Sagnac. When working with the Mach-Zehnder array, we first implemented a feedback system in order to stabilize the reference pattern. One of the two paths followed by the laser beam was used for feedback. The feedback system should allow us to compensate the jitter and thermal drifts of the fringe patterns that preclude a proper measurement of the phase shift. This requires an electronic signal, after proportional-integral amplification, to be fed to a piezotransducer in a servoloop, so as to stabilize the interferometer, thereby locking the fringe pattern. Although we succeeded in locking the fringe pattern, the geometry of our array severely limited the parameter range we could explore. We thus turned to a different option, i.e., the one based on Eqs. (16) and (17). It required polarizing one half of the laser beam in one direction and the other half in a direction perpendicular to the first one.

In order to exhibit the feasibility of our interferometric method, we performed experiments with both Mach-Zehnder and Sagnac arrays. In both cases we obtained similar preliminary results. However, the systematic recording of our results corresponds to the Mach-Zehnder array shown in Fig. 1, as it was the simpler one to mount and manipulate. As shown in the figure, the initially polarized laser beam was expanded, so that its upper half passed through one polarizer $P_1$ and its lower half through a second polarizer $P_2$ orthogonally oriented with respect to the first. Each run started by setting the retarders so as to afford the identity transformation $Q(\pi/4)H(-\pi/4)Q(\pi/4)=1_P$; the corresponding interferogram was captured with a CCD camera (1/4″ Sony CCD, video format of $640\times480$ pixels, and frame rate adjusted to 30 fps) and digitized with an *IBM*-compatible computer. The upper and the lower halves of this interferogram showed a small relative shift stemming from surface irregularities and tiny misalignments. The initial interferogram served to gauge all the successive ones that correspond to transformations $U(\xi,\eta,\zeta)\neq 1_P$. Each interferogram was evaluated with the help of an algorithm that works as follows. First, by optical inspection of the whole set of interferograms—corresponding to a given $U(\xi,\eta,\zeta)$—one selects (by pixel numbers) a common region $R_0$ of the images the algorithm should work with (see Fig. 4). Having this region as its input

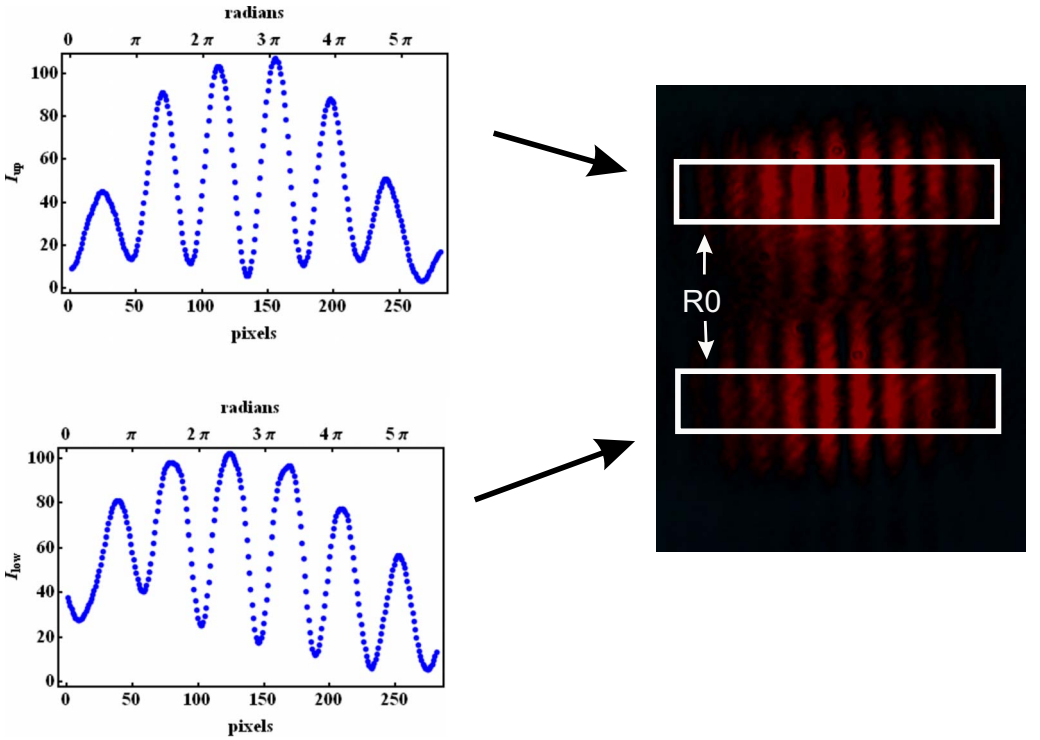


FIG. 4. (Color online) Pancharatnam's phase can be extracted from the relative fringe shift between the upper and the lower parts of the interferogram. The relative shift equals twice the Pancharatnam's phase. The left panels show the result of performing a column average of the fringes plus the application of a Savitzky-Golay filter to get rid of noise features. The column average is performed after selecting the evaluation area $R_0$ on the interferogram, as illustrated on the right panel. The reported shifts are mean values obtained from four different selections $R_0,\ldots,R_3$ of the evaluation area.

the algorithm performs a column average of each half of the interferogram—thereby obtaining the mean profile of the fringes—and the output is then submitted to a low-pass filter (Savitzky-Golay filter) to get rid of noisy features. The result is a pair of curves like those shown in Fig. 4. The algorithm then searches for relative minima in each of the two curves and compares their locations so as to output the relative shifts between the minima of the curves. After averaging these relative shifts the algorithm produces its final output for each pair of curves. We repeated this procedure for a series of regions (fixed by pixel numbers) $R_0,\ldots,R_3$, so that we could estimate the uncertainty of our experimental values. No attempt was made to automate the selection of the working regions. Visual inspection proved to be effective enough for our present purposes. Some series of interferograms showed limited regions that were clearly inappropriate for being submitted to evaluation, as they reflected inhomogeneities and other features that stemmed from surface irregularities of the optical components. We applied the complete procedure to a whole set of interferograms corresponding to different choices of $U(\xi,\eta,\zeta)$. Our results are shown in Fig. 5. As can be seen, our experimental results are in very good agreement with theoretical predictions.

A second independent, algorithm was also used to check the above results. This algorithm was developed as a variant of some commonly used procedures in image processing. Like in the previous approach, the algorithm first constructs the mean profiles of the fringes and submits them to a low-pass filter. But now, instead of searching for relative minima, the algorithm does the following. First, it determines the dominant spatial carrier frequency $k_0$ by Fourier transforming curves like those shown in Fig. 4. Let us denote these curves by $\hat{i}_{up}(x)$ and $\hat{i}_{low}(x)$, corresponding, respectively, to the upper and the lower halves of the interferogram. The Fourier transforms are denoted by $i_{up}(k)$ and $i_{low}(k)$. The goal is to determine the relative shift $\Delta_r=2\delta$ between $\hat{i}_{up}(x)$ and $\hat{i}_{low}(x)$. It can be shown [17] that $\Delta_r=\Delta_{up}-\Delta_{low}$

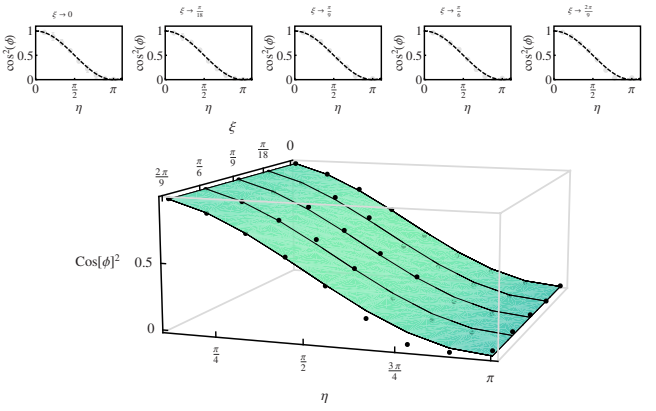


FIG. 5. (Color online) Experimental results from the interferometric measurement of Pancharatnam's phase. We plot $\cos^2(\Phi_P)$ as a function of $\xi$ and $\eta$, with $\zeta$ being held fixed to zero. In the upper panels we plot the single curves that are highlighted on the surface shown on the lower panel. Dots correspond to experimental values, some of which fall below and some fall above the surface.

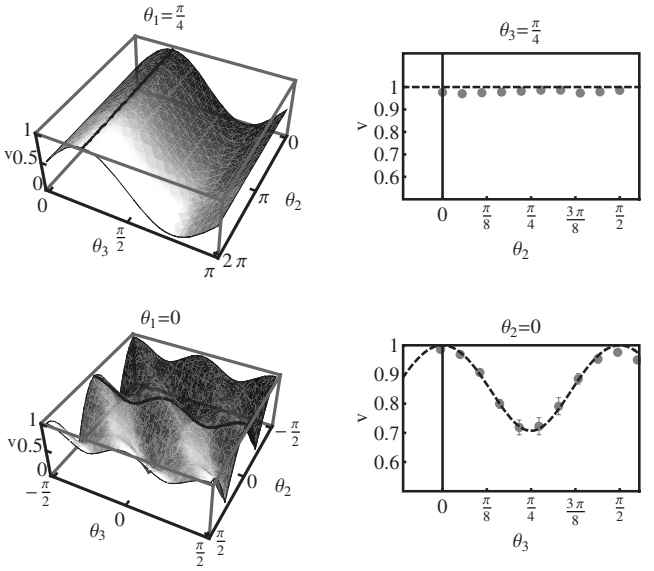


FIG. 6. Interferometric measurement of the visibility $v(\theta_1,\theta_2,\theta_3)$. The left panels show the surfaces obtained by fixing one of the three angles, $\theta_1$, as indicated. The right panels show the experimental results that correspond to the curves highlighted on the surfaces. The upper curve is obtained by fixing $\theta_3$ besides $\theta_1$, while the lower curve is obtained by fixing $\theta_2$ and $\theta_1$. In the upper curve all experimental values fall below the predicted (maximal) visibility of 1. This is because $I_{\min}$ is never zero, as required to obtain $v=1$. By subtracting the nonzero average of $I_{\min}$ the experimental points would fall above and below the theoretical curve, as it occurs for the lower curve, which corresponds to $v<1$.

$\approx \mathrm{Im}\{\ln[i_{up}(k_0)]\}-\mathrm{Im}\{\ln[i_{low}(k_0)]\}$, up to a constant phase offset that is the same for all the interferograms pertaining to a given $U(\xi,\eta,\zeta)$. The above expression for $\Delta_r$ comes from observing that both $i_{up}(k_0)$ and $i_{low}(k_0)$ have the structure $i(k_0)=a(k_0)+b(0)\exp(i\Delta)+b^*(2k_0)\exp(-i\Delta)$, so that $i(k_0)\approx b(0)\exp(i\Delta)$ whenever $|b(0)|\gg|b^*(2k_0)|,|a(k_0)|$. Thus, the accuracy of the approximation for $\Delta_r$ depends on how well one can separate the Fourier components of $i(k_0)$. In the present case we applied this procedure only for the sake of checking our results. An attempt to systematize this method would be worth only if one's goals require an automated phase-retrieval method. In our case, as we were interested in giving a proof of principle only, the method of choice was not a fully automated one, but a partially manual method which was envisioned to demonstrate the feasibility of our approach.

Another series of tests was devoted to measuring the visibility $v$ as given in Eq. (11). The quantity $v(\theta_1,\theta_2,\theta_3)$ was submitted to test by fixing two of its three arguments. Our results are shown in Fig. 6. The left panels correspond to $v(\theta_1,\theta_2,\theta_3)$ as a function of $\theta_2$ and $\theta_3$, that is, the surface obtained by fixing $\theta_1$ as indicated. In the right panels we compare the theoretical predictions against our measurements of $v(\theta_1,\theta_2,\theta_3)$, whereby two of the three arguments have been held fixed. The interferograms were evaluated following a procedure similar to the one already explained. However, in this case it was not the full cross section of the beam that was submitted to evaluation, but a manually chosen region of the images corresponding to a part of the input beam having almost uniform intensity. This had to be so, because Eq. (11) presupposes a uniform profile of the input beam. In order to test the visibility of the whole cross section of the beam, Eq. (11) should be modulated with a Gaussian envelope. Such a refinement was however unnecessary for our scopes. In any case, the experimental value of the visibility, viz., $(I_{\max}-I_{\min})/(I_{\max}+I_{\min})$, was obtained by choosing in each interferogram several maxima and minima, so as to assess the accuracy of our measurements. Thus, the error bars in the figures take proper account of the tiny variations in the chosen region of the input-beam profile. As can be seen, the experimental values closely fit the theoretical predictions.

## IV. CONCLUSIONS

We have carried out theoretical calculations and the corresponding measurements of Pancharatnam's phase by applying the polarimetric and the interferometric methods. Our interferometric array is robust against thermal and mechanical disturbances. It can be implemented with a Michelson, a Sagnac, or a Mach-Zehnder interferometer. We have compared our measurements with those obtained in a polarimetric array, finding similar results in both cases. Our polarimetric array consisted of five wave plates and two polarizers. Five plates are necessary to realize an arbitrary SU(2) transformation with the polarimetric array. As well known, three plates are instead required for realizing an arbitrary SU(2) transformation with an interferometric array. The whole Poincaré sphere of polarization states could be explored with both our polarimetric and interferometric arrays. Thus, any two given polarization states could be connected by the appropriate SU(2) transformation. The associated relative Pancharatnam's phase would thereby be realized. This phase can be decomposed as a sum of dynamical and geometrical phases. By appropriately choosing the path connecting two given states on the Poincaré sphere, one can study different aspects of both the dynamical and the geometrical phases.

We have also tested theoretical predictions concerning fringe visibility when applying the interferometric method. Our experimental findings were in very good agreement with theoretical predictions. This is interesting not only on its own, but also in view of extracting Pancharatnam's phase from visibility measurements in the case of mixed states. Indeed, it has been proved [18] that, for mixed states, fringe visibility is a simple function of Pancharatnam's phase.

## ACKNOWLEDGMENTS

We wish to thank E. J. Galvez for his technical advice and for kindly lending us some optical equipments. This work was partially supported by DAI-PUCP (Contract No. DAI-2009-0010). R.W. acknowledges financial support from the Deutsche Forschungsgemeinschaft (Contracts No. WI 393/20-1 and No. WI 393/21-1).

[1] S. Pancharatnam, Proc. Indian Acad. Sci., A **44**, 247 (1956).
[2] M. V. Berry, J. Mod. Opt. **34**, 1401 (1987).
[3] A. Tomita and R. Y. Chiao, Phys. Rev. Lett. **57**, 937 (1986).
[4] R. Bhandari and J. Samuel, Phys. Rev. Lett. **60**, 1211 (1988).
[5] T. H. Chyba, L. J. Wang, L. Mandel, and R. Simon, Opt. Lett. **13**, 562 (1988).
[6] A. G. Wagh, V. C. Rakhecha, J. Summhammer, G. Badurek, H. Weinfurter, B. E. Allman, H. Kaiser, K. Hamacher, D. L. Jacobson, and S. A. Werner, Phys. Rev. Lett. **78**, 755 (1997).
[7] A. G. Wagh, G. Badurek, V. C. Rakhecha, R. J. Buchelt, and A. Schricker, Phys. Lett. A **268**, 209 (2000).
[8] A. G. Wagh and V. C. Rakhecha, Pramana **63**, 51 (2004).
[9] A. G. Wagh and V. C. Rakhecha, Phys. Lett. A **197**, 112 (1995).
[10] A. G. Wagh and V. C. Rakhecha, Phys. Lett. A **197**, 107 (1995).
[11] V. C. Rakhecha and V. G. Wagh,Pramana, J. Phys. **56**, 287 (2001).
[12] M. Ericsson, D. Achilles, J. T. Barreiro, D. Branning, N. A. Peters, and P. G. Kwiat, Phys. Rev. Lett. **94**, 050401 (2005).
[13] R. Simon and N. Mukunda, Phys. Lett. A **143**, 165 (1990).
[14] B.-G. Englert, C. Kurtsiefer, and H. Weinfurter, Phys. Rev. A **63**, 032303 (2001).
[15] W. P. Schleich, *Quantum Optics in Phase Space* (Wiley-VCH, Berlin, 2001).
[16] R. Simon and N. Mukunda, Phys. Lett. A **138**, 474 (1989).
[17] K. A. Goldberg and J. Bokor, Appl. Opt. **40**, 2886 (2001).
[18] E. Sjöqvist, A. K. Pati, A. Ekert, J. S. Anandan, M. Ericsson, D. K. L. Oi, and V. Vedral, Phys. Rev. Lett. **85**, 2845 (2000).